Wadi Alshatti University Journal of Pure and Applied Sciences

مجلة جامعة وادي الشاطئ للعلوم البحتة والتطبيقية

Volume 3, No. 2, July-December 2025 Online ISSN: 3006-0877 المجلد 3، الاصدار 2، يوليو- ديسمبر 2025

**RESEARCH ARTICLE** **ELECTRICAL ENGINEERING**

# Reliable and Robust Optimal Interleaved Boost Converter Interfacing PhotoVoltaic Generator

Dhari A. Albuzia [1*], Alaa F. Ali[2], Mansour A. Mohmed[2], Ahmed A. Hafez[2]

[1]Distribution Grid, Capital Emergencies, Ministry of Electricity & Water, Kuwait

[2]Electrical Engineering Department, Faculty of Engineering, Assiut University, Assiut, Egypt

**ARTICLE HISTORY**

Received 30 May 2025
Revised 02 August 2025
Accepted 10 August 2025
Online 12 August 2025

**KEYWORDS**

Interleaving;
Boost;
Optimization;
GOA;
Ripples

**ABSTRACT**

This article introduces a simple and reliable interleaved boost converter that interfacing photovoltaic (PV) generator. The PV generator is driven at Maximum Power Point (MPPT) via Perturb and Observe (P&O) algorithm. A simple control strategy based on a Proportional-Integral (PI) controller is advised to control the boost chopper and the PV generator. PI improves the dynamic performance, reduce the steady-state error, and increase the robustness against nonlinearities and parameter variations. The controller parameters are optimally tuned using the bio-inspired Goose Optimization Algorithm (GOA), which exhibits fast convergence and high efficiency in complex optimization tasks. The simulation studies corroborate the proposed ability of the system to maintain constant DC link voltage, accurately track current references, and achieve high power conversion efficiency under dynamic operating conditions.

## مغير تعزيز متداخل مثالي موثوق وقوي يوصل مولد الطاقة الكهروضوئية

ضاري عبدالمحسن [1,*]، علاء فرح [2]، منصور أحمد محمد [2] ، أحمد عبدالمالك عبدالحافظ [2]

**الكلمات المفتاحية**

التداخل
التعزيز
التحسين
*GOA*
التموجات

**الملخص**

تُقدّم هذه المقالة مُحوّل تعزيز مُتداخل بسيط وموثوق، يعمل على ربط مُولّد الطاقة الكهروضوئية (PV). يُشغّل مُولّد الطاقة الكهروضوئية عند نقطة القدرة القصوى (MPPT) عبر خوارزمية الاضطراب والمراقبة (O&P). يُنصح باستخدام استراتيجية تحكم بسيطة تعتمد على مُتحكّم تناسبي-تكاملي (PI) للتحكم في مُفرّغ التعزيز ومُولّد الطاقة الكهروضوئية. يُحسّن مُتحكّم التناسب-التكامل (PI) الأداء الديناميكي، ويُقلّل خطأ الحالة المستقرة، ويُعزّز المتانة في مواجهة اللاخطية وتغيّرات المُعاملات. تُضبط مُعاملات المُتحكّم على النحو الأمثل باستخدام خوارزمية تحسين *Goose (GOA* المُستوحاة من علم الأحياء، والتي تُظهر تقاربًا سريعًا وكفاءة عالية في مهام التحسين المُعقّدة. تُؤكّد دراسات المحاكاة القدرة المُقترحة للنظام على الحفاظ على ثبات جهد وصلة التيار المُستمر، وتتبع مراجع التيار بدقة، وتحقيق كفاءة تحويل طاقة عالية في ظلّ ظروف التشغيل الديناميكية.

## Introduction

PV and wind turbine generators (WTGs) are two examples of renewable energy sources (RESs) that are being used more and more to lessen dependency on the utility grid [1]. RESs in general enjoy the environmental computability, sustainability and availability. RESs could be an acceptable alternative for the fossil fuels in generating electricity. PV has the power and size variability; they could be available down from 1W. PV and RESs in general suffer from uncertainty and climatological dependence.

DC–DC converters are frequently used to adjust output voltage and reduce current ripples, they still encounter challenges such fluctuating loads, input disruptions, and control constraints like pulse-width modulation (PWM) saturation. Boost converter has the ability to interface a low voltage source as PV to high voltage DC link. The boost converter is best alternative for interfacing PV generator. The boost diode ensures full protection of the PV generator as it prevents the generator from acting as load under abnormal operating conditions as shading and faults [2,3].

In [4] a comparison between the basic cell boost converter and the interleaved topology is presented. The interleaving concept is highly advisable for high-power applications, where two or more identical converters are connected in parallel. The [4] claim that the interleaved boost converter implemented PV system has comparatively more minor ripples than standard boost converter implemented PV systems which tends to reduce losses and output filter size. However, [4] has not pay much attention to the MPPT. Moreover, nor practical setup is advised or varying solar irradiance is considered.

Ref [5] presents the design, analysis and modelling of a smart heating system for solar PV Electric Vehicle (EV) charging applications. The system is based on a bidirectional DC-DC converter that redirects the grid/EV-battery power into heating of the solar PV modules, thus removing snow cover, as well as providing the function of MPPT when required to charge the EV battery pack. A control scheme for each mode of operation was designed.

In [6], charging of EV via interleaved boost converter is advised. The PV generator is interfaced to the Lithium Ion battery via the interleaved boost chopper. Charging of the

*Corresponding author
https://doi.org/10.63318/waujpasv3i2_24

multiple EV batteries is realized via the distributed phase-shift full bridge converters. The battery charging process is controlled by the constant current-constant voltage (CC-CV) technique to align with the requirements of the battery. However, [6] has not considered the operation under varying levels of solar irradiance.

Ref. [7] proposes a renewable energy - based propulsion system for EVs using boost chopper and an optimized MPPT approach. The PV system provides power that is allowed the interleaved chopper to current sharing between stages, which reduces the thermal stress on individual components, improving reliability. An MPPT based on Whale Optimization Algorithm (WOA) tracks the maximum power point more precisely. After converting the incoming DC power, the 3-phase Voltage Source Inverter (VSI) provides AC to the three-phase source. A Brush Less DC (BLDC) motor is achieved by the power use of a PI controller. The simulation is implemented in MATLAB Simulink. In contrast to WOA techniques, the results indicate that the proposed system offers excellent performance and improves the overall system efficiency. However, the operation under different climatological conditions is not considered.

In [8], the integration of solar panels into standalone applications using a high-gain DC-DC converter coupled with an MPPT controller is proposed. Specifically, a non-isolated interleaved quadratic boost converter topology serves as the DC-DC converter for the charge controller implementation. The Perturb and Observe method is the MPPT algorithm used, and it tracks the solar panel's maximum power. The performance of a high-gain converter, designed with specifications for 600W, 16/400V, and a 40KHz switching frequency, is validated through simulation . The article claim that the proposed circuit achieves an efficiency of 94.53%.

Different interleaved converters are considered for interfacing PV systems into EVs and or different loads [2-10]. The interleaved boost topology is the most promising candidate, since the inductors are in the input side. Therefore, the reduce the ripple in the current drawn from the PV converters [9, 10].

Numerous control systems, from traditional voltage and current mode control to sophisticated and intelligent techniques, have been developed to handle these problems. While techniques such as model predictive control (MPC), fuzzy logic control (FLC), and sliding mode control (SMC) have demonstrated enhanced dynamic response and regulation capabilities, each has trade-offs with respect to system complexity, scalability, and sensor requirements for high-power applications [2-10].

The GOA emulates the cooperative and migratory behaviour of geese flying in V-shaped formations. It is a bio-inspired metaheuristic optimization technique. In order to improve the effectiveness and resilience of the search process, this algorithm simulates important facets of geese dynamics, including as coordinated movement, group cohesion, leader-follower interaction, and periodic leadership rotation. Each geese in the computational environment is a possible solution in the search space, and its location is iteratively updated by the centroid of the group, the best-performing leader in its group, and stochastic perturbations that encourage exploration. By skillfully striking a balance between local exploitation and global exploration, the algorithm can traverse intricate, multimodal, high-dimensional optimization environments. Due to its structured population division and adaptive information-sharing strategy, GOA has demonstrated strong convergence behavior and high optimization performance in various engineering and scientific applications [12].

In this article, the interleaved AC/DC boost-converter is used to interface a PV generator. By addressing issues such as high input and output ripples, this converter technology ensures a smoother and more stable power transfer. The interleaved configuration allows for the distribution of current across multiple phases, minimizing stress on individual components and promoting a more balanced system operation. The article is claiming to achieve the following contributions:

1. Proposes an efficient PV-based power system using an interleaved boost converter to reduce ripple and enhance power quality.
2. Introduces a simple and robust PI controller for bidirectional DC-DC conversion,
3. Employs GOA for optimal controller tuning and improved dynamic response.

The structure of the article is as follows: The layout of the system under concern is illustrated in Section 2. Section 3 introduces the control of the proposed PV system including the tuning of the controller. The transient performance of the interleaved boost converter interfacing a PV generator is given in Section 4. The conclusions of the article are given in Section 5.

## Layout of the System under Concern

The system under concern, Fig.1, is composed of a PV generator , interleaved boost chopper and load. The PV generator is driven at MPP via the boost converter. The load could be a battery for EV applications or other load configurations for different applications,

,

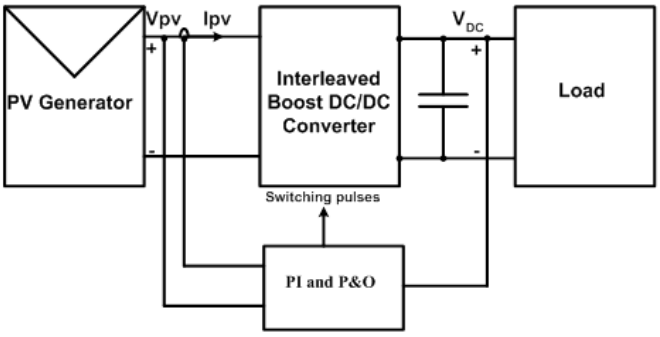


**Fig. 1**: Layout of the system under concern

## Static performance of the PV generator

The PV generator has 50 kWp, making it suitable for residential structures. It consists of 126 SPR-435NE-WHT-D PV modules. Table 1[11] contains the details of each module

**Table 1**: Parameters of module SPR-435NE-WHT-D at 25°C and 1000Wm$^2$[11].

| Items | Values |
|---|---|
| **No. of cells** | 132 |
| **Short circuit current, $I_{sc}$** | 6.43 A |
| **Open circuit voltage, $V_{oc}$** | 85.6 V |
| **Current at MPP, $I_{mpp}$** | 5.97 A |
| **Voltage at MPP, $V_{mpp}$** | 72.9 V |
| **Maximum power, $P_{mpp}$** | 435 W |
| **Temperature voltage coefficient** | -235.5m V/K |
| **Temperature current coefficient** | 3.5m A/K |
| **Cell Efficiency** | 22.40% |
| **Panel Efficiency** | 20.10% |
| **Area of Panel** | 2.16 m$^2$ |

As illustrated in Fig. 2, the PV cell/module is displayed as a temperature-dependent current source $I_{ph}$ parallel to a diode and solar irradiation. The literature [11] refers to this model as a single-diode PV model, which has the advantages of straightforwardness and reasonable accurateness. However, because of the significant power losses brought on by the existence of parallel resistors, this research disregards the parallel resistor present in the literature model [11]. In the ideal module, Rs would be zero, meaning there would be no additional voltage drop before the load, and a parallel resistance would be infinite, providing no alternative path for current flow [11].

Given the photocurrent $I_{ph}$, diode reverse current $I_o$, thermal voltage $V_{th}$, and series resistance $R_s$, the relationship between the terminal current and voltage is as follows :

$$I_t = I_{ph} - I_o\left\{e^{\left(\frac{V_t+IR_s}{V_{th}}\right)} - 1\right\} \quad (1)$$

Iterative calculations in [11] yielded a value of 0.025 Ω for the series resistance Rs. The PV generator is constructed using PV modules coupled in a series-parallel fashion. In total, 132 modules make up the PV generator. Regarding open-circuit voltage $V_{oc}$ and short-circuit current $I_{sc}$ the relation between the PV array/generator terminal voltage $V_{pv}$ and current $I_{pv}$ is as follows:

$$I_{pv} = M_s I_{sc}\left\{1 - exp\left(\frac{V_{pv} - N_s V_{oc} + N_s I_{pv} R_s/M_s}{N_s V_{th}}\right)\right\} \quad (2)$$

It is assumed that $M_s$ and $N_s$, which stand for the number of shunt and series-connected modules, respectively, are 1 and 2. Currents for photovoltaic $I_{pv}$ and $I_{sc}$ applications vary linearly with solar irradiance [11]. As a result, the power produced by the PV array varies linearly with solar irradiation. Temperature, irradiation level, and climatic operating circumstances affect the PV cell, module, and array output. The characteristic curves of the PV generator plotted at various irradiation levels and 25°C are Fig. 3 (a) (I-V) and (b) (P-V).

Fig. 3 shows that the current of the PV generator and hence its power are directly related to the solar irradiance. They almost vary in linear fashion. Fig. 4 (a) shows the I-V and (b) shows the P-V curves of solar cells plotted at 1 kW/m$^2$ and at various temperature levels.

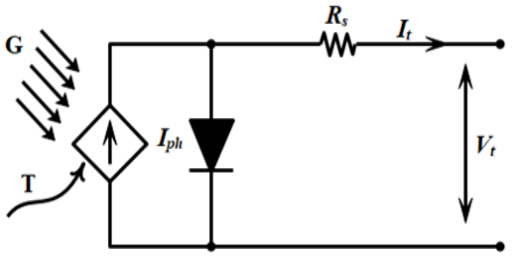


**Fig. 2:** PV equivalent circuit (single-diode model)

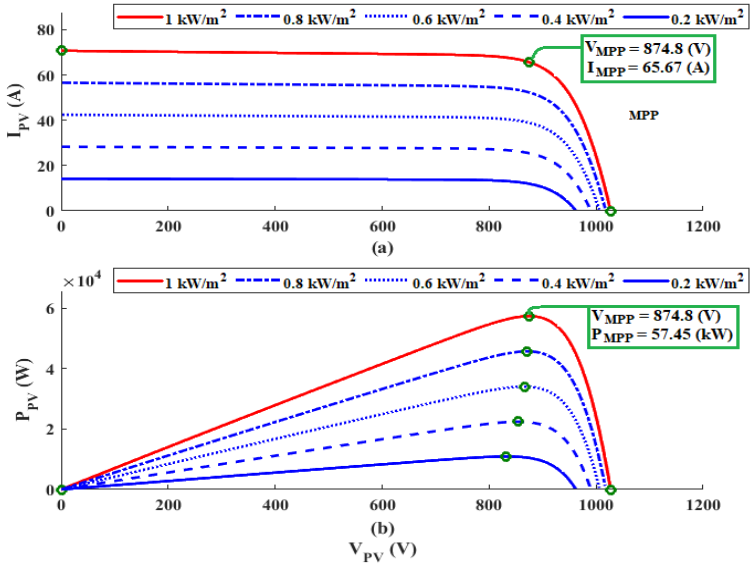


**Fig. 3: (a)** I-V and **(b)** P-V show the solar panel's characteristic curves plotted at various irradiation levels and 25°C

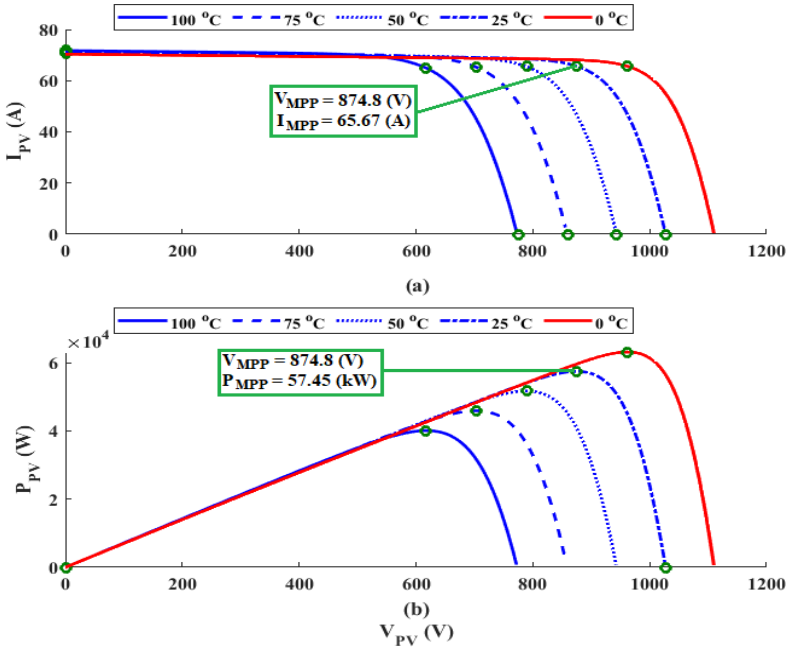


**Fig. 4**: (a) I-V and **(b)** P-V at 1 kW/m$^2$ and at various temperature levels

Fig. 4 shows that the open circuit voltage of the PV generator decreases as the temperature increases. Also, the PV output power decreases with the increase of the temperature that requires better cooling for the PV generator. Moreover, it is recommended that the PV generator function with minimum losses. Therefore, the driving DC chopper should enjoy the characteristic of high-quality input current. The boost converter, therefore, is the most promising candidate.

## Interleaved Boost Converter

The basic boost cell usually suffers from relatively high ripple content in the input current, which is not relevant for interfacing PV generator. Therefore, the proposed is using interleaved-boost converter as shown in Fig. 5. The converter is composed of two parallel basic boost converters. It has two input inductors attached to the same point, two switches and two diodes

### Operation mode of converter

Table 2 lists the four modes of the interleaved converter for the duty cycle, $\delta > 0.5$. This is ensure continuous conduction mode for the currents of the inductors, which reduces the ripples in the input current of the converter and hence the ripples in the PV generator current

The schematic of the inductor current waveforms of the converter are shown in Fig.6. Figs.7 to 10 depict the corresponding circuits for the various switching states.

**Table 2 Interleaved operation switching states - operating modes**

| Circuit Switching Mode | Switching State | $S_1$ | $S_2$ | $D_1$ | $D_2$ |
|---|---|---|---|---|---|
| Mode (I) | $\mathbf{0 < t < \delta_1 T_s}$ | **ON** | **OFF** | **OFF** | **ON** |
| Mode (II) | $\delta_1 T_s < \mathbf{t} < \delta_2 T_s$ | **ON** | **ON** | **OFF** | **OFF** |
| Mode (III) | $\delta_2 T_s < \mathbf{t} < \delta_3 T_s$ | **OFF** | **ON** | **ON** | **OFF** |
| Mode (IV) | $\delta_3 T_s < \mathbf{t} < \delta_4 T_s$ | **OFF** | **OFF** | **ON** | **ON** |

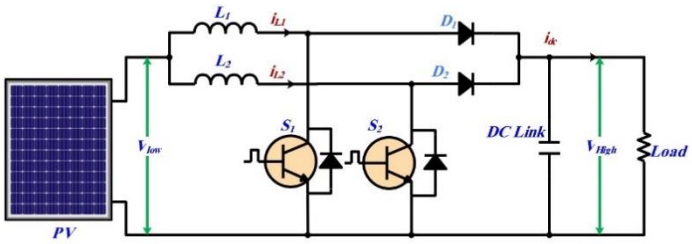


**Fig. 5:** Interleaved boost converter interfacing PV generator

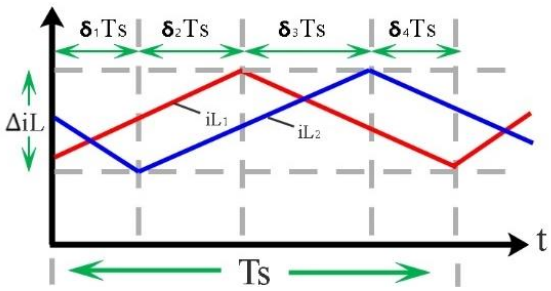


**Fig. 6:** Waveforms of the inductor currents

***Mode (I) :***(0 < t < $\delta_1$Ts) Switches S1 and D2 are in the on and off states, respectively, and the inductor's current $i_{L1}$ rises as $V_o/_2 > V_m$ $(\delta > 1/_2)$. A schematic depicting the conduction path at this phase is shown in Fig 5.

$$\begin{cases} v_{L1} = v_{in\_low} \\ v_{L2} = v_{in\_low} \end{cases} \quad (4)$$

$$v_{L1} = L_1 \frac{\delta i_{L1}}{\delta t} \text{ and } v_{L2} = L_2 \frac{\delta i_{L2}}{\delta t} \quad (5)$$

$$\frac{\delta i_{L1}}{\delta t} = \frac{|v_{in\_low}|}{L_1} \quad (6)$$

$$\frac{\delta i_{L2}}{\delta t} = \frac{|v_{in\_low}|}{L_2} - \frac{v_{out\_high}}{L_2} \quad (7)$$

***Mode (II)***: ( $\delta_1 T_s$< t < $\delta_2 T_s$): D1 and D2 are in the off state, whereas switches S1 and S2 are in the on state. The slope of the inductor currents, , $i_{L1}$ and $i_{L2}$, is positive. Figure 6 depicts the conduction path at this point:

$$\frac{\delta i_{L1}}{\delta t} = \frac{|v_{in\_low}|}{L_1} \quad (8)$$

$$\frac{\delta i_{L2}}{\delta t} = \frac{|v_{in\_low}|}{L_2} \quad (9)$$

***Mode (III)***: ( $\delta_2 T_s$< t < $\delta_3 T_s$): Switches S1 and D1 are in the off state, whereas S1 and D2 are in the on state. Because of its discharge and energy provision to the load, the inductor $L_1$ is presently down turning. Nearly simultaneously, an energy source is supplied to the inductor $L_2$ , increasing the inductor $i_{L2}$'s current. As a result, the slopes of the inductor current, $\delta i_{L1}/\delta t$ and $\delta i_{L2}/\delta t$, are, respectively, negative and positive. The conduction paths shown in Fig. 8.

$$\frac{\delta i_{L1}}{\delta t} = \frac{|v_{in\_low}|}{L_1} - \frac{v_{out\_high}}{L_1} \quad (10)$$

$$\frac{\delta i_{L2}}{\delta t} = \frac{|v_{in\_low}|}{L_2} \quad (11)$$

***Mode (IV):*** ( $\delta_3 T_s$< t < $\delta_4 T_s$): switch S1 and switch S2 are off state and D1, D2 are on state. This causes both $L_1$ and $L_2$ inductors to discharge and supply the load with energy this leads to a lowering in the current $i_{L1}$ and $i_{L2}$ inductor. Consequently, the slopes of the inductor current are both negative. Fig 10 displays this schematic.

$$\frac{\delta i_{L1}}{\delta t} = \frac{|v_{in\_low}|}{L_1} - \frac{v_{out\_high}}{L_1} \quad (12)$$

$$\frac{\delta i_{L2}}{\delta t} = \frac{1}{1-\delta} - \frac{v_{out\_high}}{L_2} \quad (13)$$

The duty cycle of the interleaved converter , δ , is given by (14):

$$\frac{v_{out\_high}}{v_{in\_low}} = \frac{1}{1-\delta} \quad (14)$$

**The Control of PV Generator based Boost Chopper**

The control of the PV generator driven by interleaved boost converter is shown in Fig. 11. The control consists of three layers. The objectives of the control are:

- Driving the PV generator at MPPT under varying climatological conditions that involves rapid change for solar irradiance
- Reducing the ripples in the currents of the inductors and hence the input current of the interleaved boost chopper.

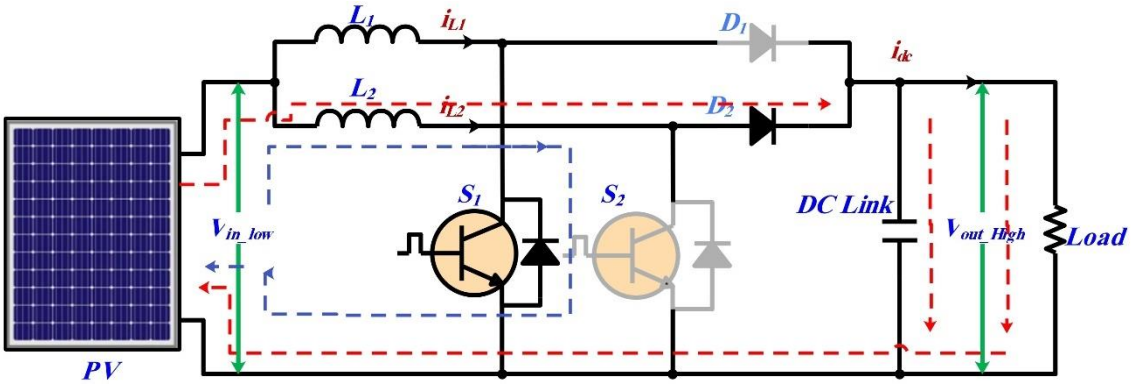


**Fig. 7:** Equivalent circuit during mode (I)

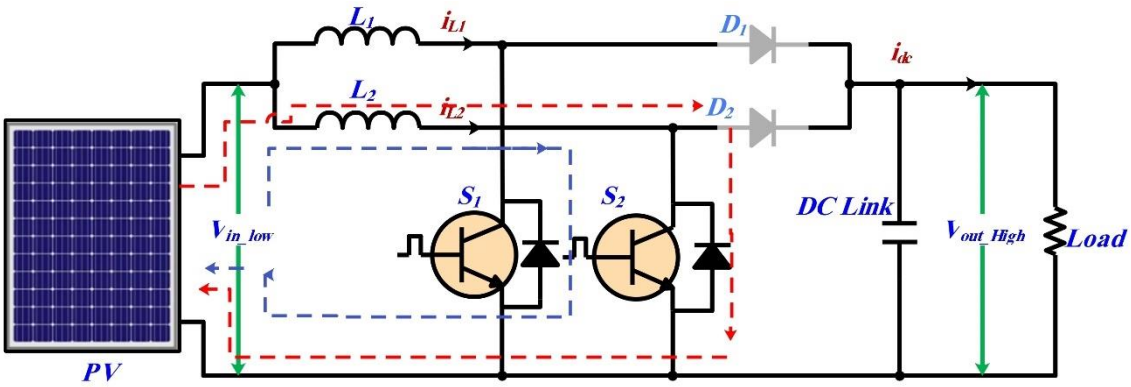


**Fig. 8:** Equivalent circuit during mode (II)

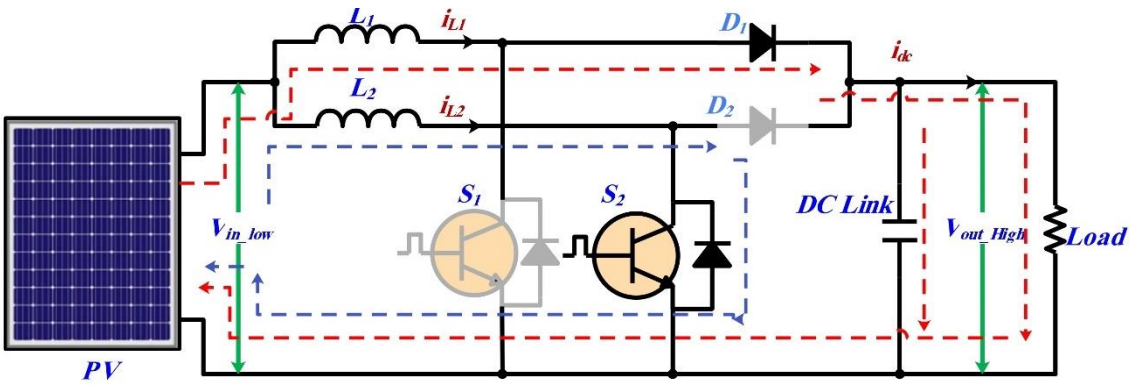


**Fig. 9:** Equivalent circuit during mode (III)

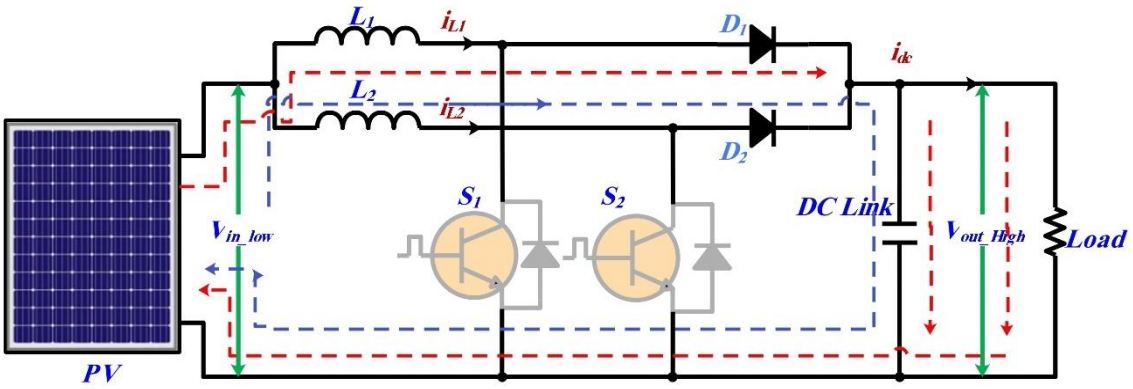


**Fig. 10:** Equivalent circuit during mode (IV)

The block diagram ,Fig. 11, shows that the MPPT generate the reference signal for the voltage loop . The voltage loop generates the references. A PI controller is used in each layer. In general, the PI controller is defined by:

$$U(s) = \left(\left(k_p + k_i.S^{-1}\right)\right) * E(s) \quad (15)$$

Where, $k_p$ is the proportional gain, $k_i$ is the integral gain. E is the input for the PI controller, which is the error between the controlled and actual signals. U is the output of the PI controller

**Tuning of the Controller**

GOA matches the cooperative and migratory behavior of geese flying in V-shaped formations. It is a bio-inspired metaheuristic optimization technique. GOA is used in this research to find the optimal parameters of the PI controller [12]. The flowchart of GOA used for determining the optimal parameter for the controller is shown in Fig. 12.

The GOA minimize the objective function

$$minimize(Fc), where\ Fc = E_1(s) + E_2(s) + E_3(s)(s) \quad (16)$$

where the $k_i$ and $k_p$ of $E_1(s)$, $E_2(s)$ and $E_3(s)$ are subjected to

$$k_{p_{min}} \leq k_{pi} \leq k_{p_{max}}$$

$$k_{i_{min}} \leq k_{ii} \leq k_{i_{max}}$$

The values of $k_{p_{min}}$, $k_{i_{min}}$ and $k_{d_{min}}$ are set to -50, while $k_{p_{max}}$ , $k_{i_{max}}$ and $k_{d_{max}}$ are set to 50. The values of the different controllers optimized by GOA are given in Table 3.

**Table 3:** The optimal Parameters of the PI **controllers**

| | Parameters | values |
|---|---|---|
| PI Controller 1 | $K_{p1}$ | 19.9934 |
| | $K_{i1}$ | 1.79984 |
| PI Controller 2 | $K_{p2}$ | 20 |
| | $K_{i2}$ | 5.5719e-06 |
| PI Controller 3 | $K_{p3}$ | 0.0405798 |
| | $K_{i3}$ | 20 |

Table 3 provides values of the controllers shown in Fig.11

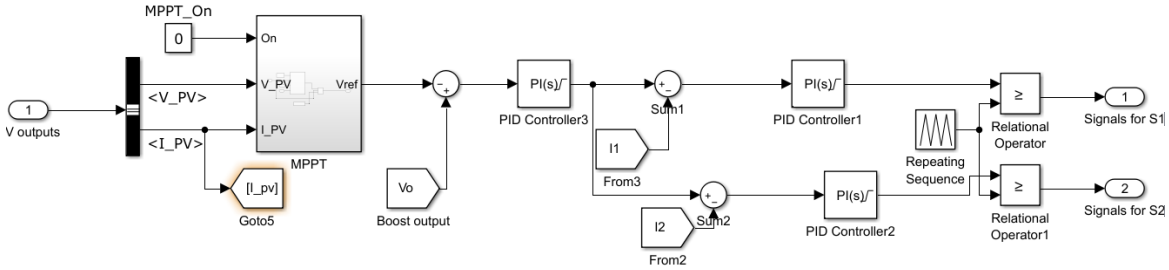


**Fig. 11:** block diagram of the proposed control for the PV generator driven via boost chopper

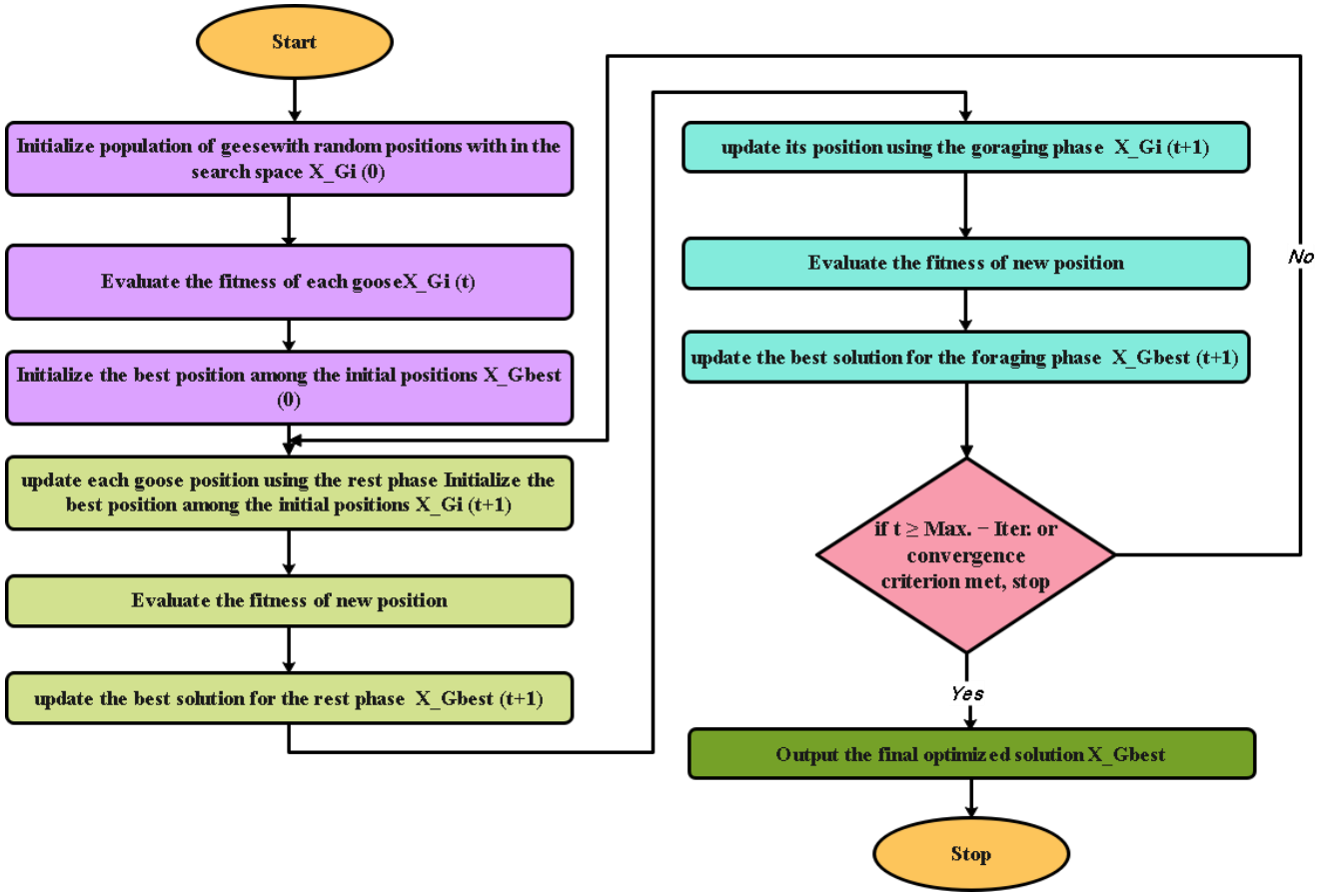


**Fig. 12:** Flow chart of GOA algorithm

**Transient Performance**

The proposed system in Fig. 1 with the parameters given in Table 4 and the controllers in Fig.11 are simulated using Simulink platform in Matlab for different levels of solar irradiances.

Fig. 13 shows the solar irradiance that stepped from 1000Wm$^{-2}$ into 500 1000Wm$^{-2}$. The figure shows also the voltage and the current of the PV generator accoridingly.

**Table 4:** Parameters of the proposed system

| Parameters | Symbol | Value |
|---|---|---|
| PV Power | $P_{pv}$ | 50kW |
| PV voltage | $v_{pv}$ | 420 |
| PV current | $I_{pv}$ | 120 |
| inductor | $L_1, L_2$ | 5e-3 |
| Dc link capacitance for PV | $C_1$ | 1000e-6 |
| DC-link capacitance for load | $C_2$ | 400e-6 |
| Load | $R_L$ | 5 ohm |
| DC voltage | $v_{dc}$ | 500 v |
| Switching frequency | $f_s$ | 10kHz |

Fig 13 illustrates the dynamic performance of PV system under varying irradiation levels. Top graph in Fig. 13 displays the irradiation profile, which undergoes changes at specific time intervals, decreasing from 1000 W/m² to 500 W/m² then stepping back to 1000 W/m². This is step the ability of MPPT technique in coping with instantaneous change in the solar irradiance. Middle graph in Fig. 13 shows the corresponding PV voltage ,Vpv, which responds to the irradiation fluctuations, indicating effective tracking for MPP. In the bottom graph, the PV current ,Ipv , responds proportionally to changes in irradiation, decreasing with reduced solar input and increasing as irradiation rises.

Fig. 14 shows the PV and load powers , load voltage and load current for varying solar irradiance shown in Fig. 13.

Fig 14 , top graph, shows the powers of the PV generator and the load. The converter efficiency is around 98%. Middle graph in Fig. 14 illustrates the load current; it varies with the solar irradiance. In the bottom graph in Fig.14, load voltage is illustrated. The load parameters, voltage and current, are responding to changes in irradiation, decreasing with reduced solar input and increasing as irradiation rises. The converter mainly drives the PV generator at MPP while reducing the losses via the interleaving action.

Fig. 15 shows the input converter of the interleaved converter and the current in each inductor for varying solar irradiance shown in Fig. 13.

Fig 15 , top graph, shows the current of the interleaved converter. It clear that the ripple content in the current is much lower than that in the individual inductor. Middle graph in Fig. 15 illustrates the current of cell 1; it varies with the solar irradiance. In the bottom graph in Fig.15, the current of the converter second cell is illustrated. The currents either input and cells' currents are responding to changes in irradiation, decreasing with reduced solar input and increasing as irradiation rises. The interleaved converter successfully reduces the ripple content of the input current, which reduces the ripples in the PV generator current and hence the losses in the PV generator.

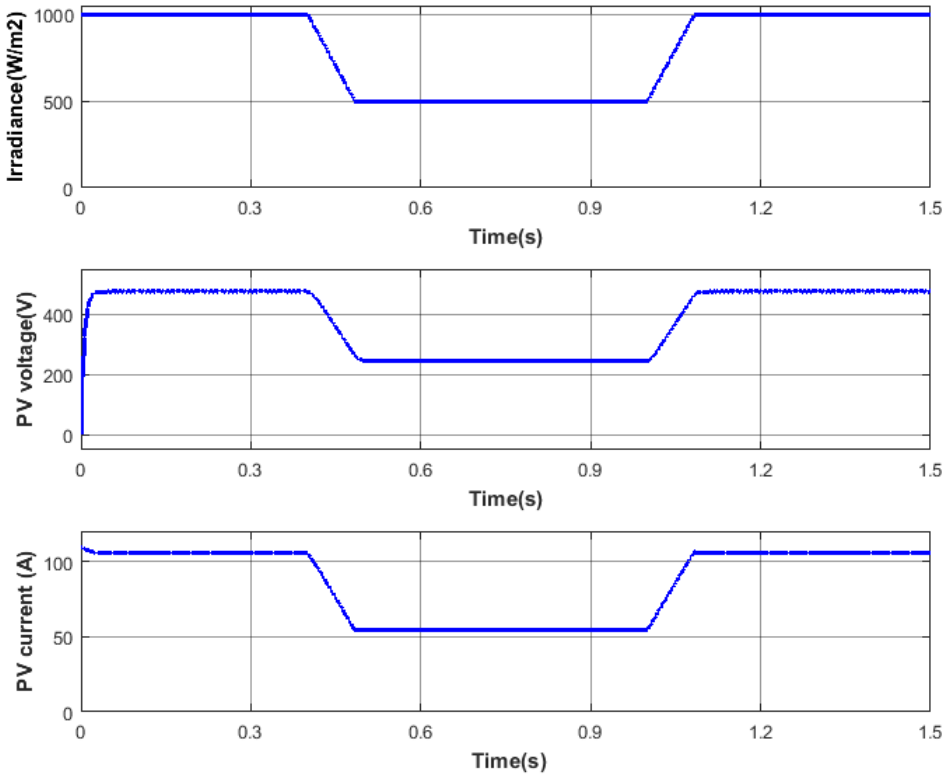


**Fig. 13:** Solar irradiance (top graph), PV voltage (middle graph), PV current (bottom graph)

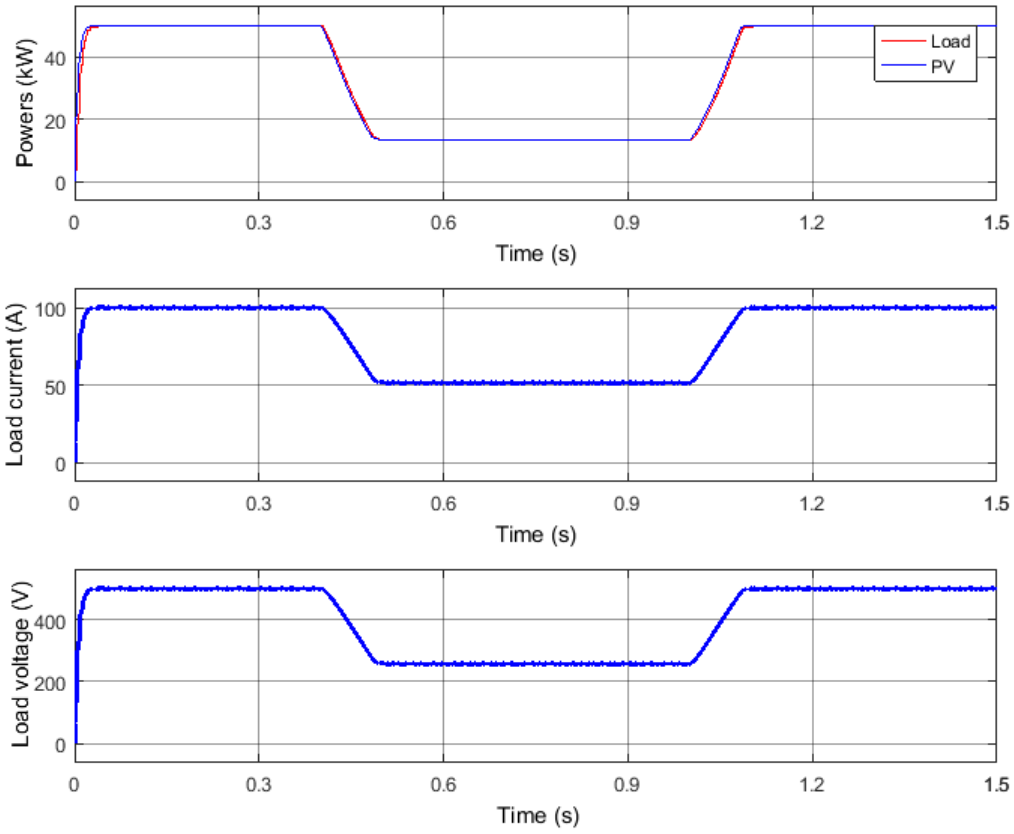


**Fig. 14:** Powers (top graph, blue : PV power, red: load power), load current (middle graph), load voltage (bottom graph)

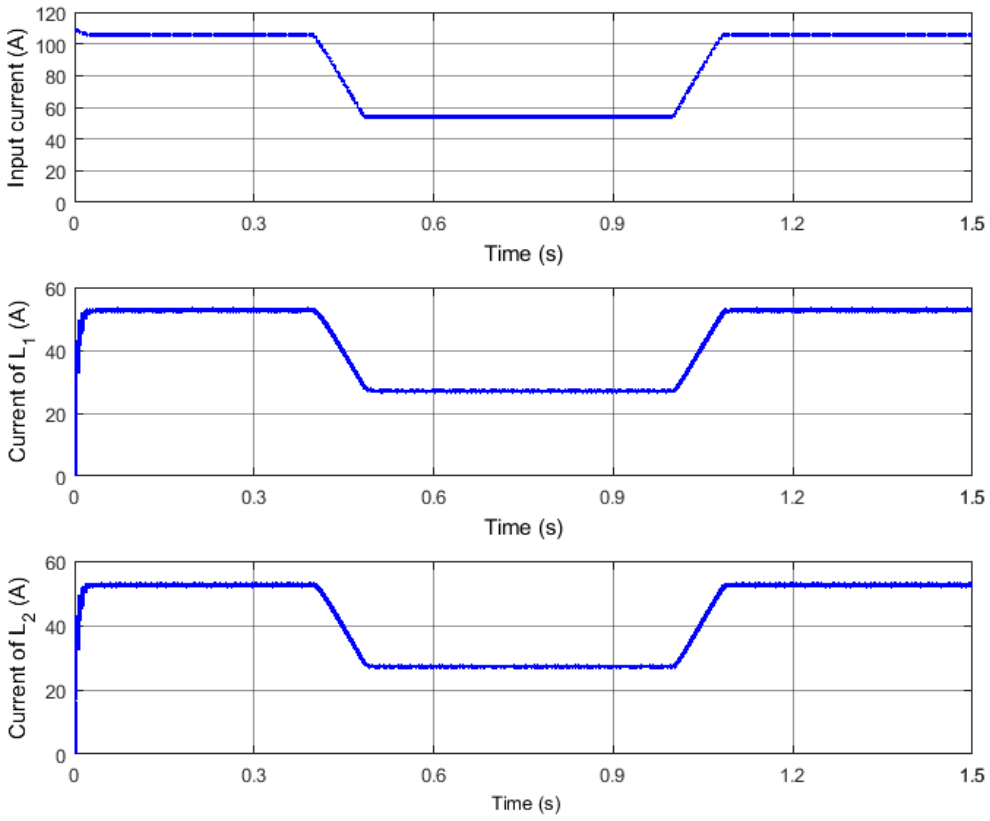


**Fig. 15:** Converter input current (top graph), current of inductor $L_1$(middle graph), current of inductor $L_1$ (bottom graph)

## Conclusion

PV technology is progressively spreading due to inconveniences of fossil fuels. However, PV systems suffer from uncertainty and climatological dependence. Moreover, the performance of the PV systems is affected by the losses. Therefore, the driving converters/circuits have to consider such operating conditions. A simple and reliable interleaved boost converter that interfacing photovoltaic a PV generator is proposed. The PV generator is driven at MPPT via P&O algorithm. A PI, tuned via GOA is used to drive the system. The proposed PI improves the dynamic performance, reduce the steady-state error, and increase the robustness against nonlinearities and parameter variations.

The simulation results validate the proposed ability of the system to maintain constant DC link voltage, accurately track current references, and achieve high power conversion efficiency under dynamic operating conditions. The results demonstrate that the proposed system maintains stable voltage and current regulation across a wide range of irradiance levels. The interleaved converter architecture effectively minimized current ripple, improved thermal distribution, and enhanced overall system reliability.

**Author Contributions**: “Conceptualization, methodology, and writing—original draft preparation are carried out by Albuzia. Reviewing of the analysis is carried out by Hafez, review and editing are carried out by Farah, Mohamed and Hafez. All authors have read and agreed to the published version of the manuscript.”

**Funding**: “This research received no external funding.”

**Data Availability Statement**: “The data are available at request OR Not applicable.”

**Acknowledgments**: "The authors would like to express their appreciation to the Electrical Engineering Department, Faculty of Engineering, Assiut University, Assiut, Egypt"

**Conflicts of Interest**: “The authors declare no conflict of interest."

## References

[1 ] S. Ahmad, A. Agrira, and N. Fathi/ "The Impact of Loss of Power Supply Probability on Design and Performance of Wind/ Pumped Hydropower Energy Storage Hybrid System." *Wadi Alshatti University Journal of Pure and Applied Sciences*, vol. 3, no. 2, pp. 52-62, 2025. https://doi.org/10.63318/waujpasv3i2_06

[2 ] R. Gopalasami and B. Chokkalingam, “A Photovoltaic-Powered Modified Multiport Converter for an EV Charger with Bidirectional and Grid Connected Capability Assist PV2V, G2V, and V2G,” World Electr. Veh. J., vol. 15, no. 1, 2024, doi: 10.3390/wevj15010031.

[3 ] K. Swamynathan, N. Mahalingam, A. Paramasivam, and S. Vijayalakshmi, “PV based OFF grid charging station for E-vehicles using PWM and phase shift controlled interleaved three port converter,” SN Appl. Sci., vol. 5, no. 12, 2023, https://doi.org/10.1007/s42452-023-05571-w.

[4 ] R. Ruchika, S. Gauta, M. Kumar. "Comparative Analysis of Boost and Interleaved Boost Converter for PV Applicatio n" 2022 2nd International Conference on Emerging Frontiers in Electrical and Electronic Technologies (ICEFEET), pp. 1-6, 2022. https://doi.org/10.1109/ICEFEET51821.2022.9848264

[5 ] S. Aviles, A. Kadam, T. Sidhu, and S. Williamson, “Modeling, Analysis, Design, and Simulation of a Bidirectional DC-DC Converter with Integrated Snow Removal Functionality for Solar PV Electric Vehicle Charger Applications,” Energies, vol. 15, no. 8, 2022. https://doi.org/10.3390/en15082961.

[6 ] A.Rawat; and R. Gupta."Interleaved Boost Converter Based Solar PV Plant for Distributed Battery Charging." 2023 9th IEEE India International Conference on Power Electronics

(IICPE), pp. 1-8, 2023. https://doi.org/10.1109 /IICPE60303.2023.10475058

[7 ] C. Robin, J. Raji, M. Yaseen, N. Jothippriya, M. Irfan, I. Shivasankkar. "Interleaved Boost Converter with Optimized MPPT Approach for Renewable Energy Based Propulsion System of EV." 2025 3rd International Conference on Device Intelligence, Computing and Communication Technologies (DICCT), pp. 1-7, 2025. https://doi.org/ 10.1109/DICCT64131.2025.10986565

[8 ] R. Kalyani, P. Raviteja, and B. Narasimharaju. "Solar PV Integrated MPPT Controlled High Gain DC-DC Converter." 2024 IEEE 4th International Conference on Sustainable Energy and Future Electric Transportation (SEFET), pp. 1-9, 2024. https://doi.org/10.1109/ SEFET61574.2024.10718155

[9 ] A. Rawat, and R. Gupta."Standalone Solar PV Plant for Distributed Battery Charging Using PSFB and DAB." 2024 IEEE Students Conference on Engineering and Systems (SCES), pp. 10-20, 2024. https://doi.org/10.1109/ SCES61914.2024.10652484

[10 ] V. Bhasker, A. Mishra. "Solar PV Powered Electric Vehicle Charger Based on ISSB Converter with Ripple Cancellation Circuit." 2024 IEEE Third International Conference on Power Electronics, Intelligent Control and Energy Systems (ICPEICES), pp. 1-8, 2024. https://doi.org/10.1109/ ICPEICES62430.2024.10719243

[11 ] A. Sharma, K. Gupta, K. Jangir, P. Jain and P. Malakar, "Multi-objective Greylag Goose Optimization," 2 2024nd International Conference on Advancement in Computation &Computer Technologies (InCACCT ,(Gharuan, India, 2024, pp. 374-379, https://doi.org//10.1109InCACCT61598. 2024.10551106 .

[12 ] SunPower, “SunPower E20 / 435 SOLAR PANEL.” 2025, https://www.energysage.com/equipment/solar-panels/sunpower/spr-e20-435-com-de774dc2/